

EISS: an HF mono and bistatic GPR for terrestrial and planetary deep soundings

M. Biancheri-Astier, R. Hassen-Khodja, V. Ciarletti,
C. Corbel, Y. Simon, C. Caudoux, J. Faroux, F. Dolon,
V. Leray

Laboratoire Atmosphère, Milieux, Observations Spatiales
University of Versailles St-Quentin ; CNRS/INSU,
LATMOS-IPSL, France
mbi@latmos.ipsl.fr - rhk@latmos.ipsl.fr

A. Reineix
XLIM institut de recherche
University of Limoges / CNRS, France

D. Plettemeier
Institute for High-Frequency
University of Bochum, Germany

Abstract— EISS (Electromagnetic Investigation of the SubSurface) is an HF (~2MHz) impulse Ground Penetrating Radar dedicated to deep soundings (kilometric depths) of planetary sub-surfaces. This radar has the particularity to be operated from the surface in both monostatic (transmitter and receiver at the same location) and bistatic configurations (with a small receiver separated from the transmitter that can easily be displaced on the area to be investigated). A prototype has been developed in the frame of ExoMars mission B-phase. This article mainly focuses on the bi-static mode and details the selected design, its various subsystems and its operations. Preliminary tests involving antenna impedance measurements on Earth are shown.

Keywords— Ground Penetrating Radar, deep sounding, wave propagation, subsurface, bistatic, monostatic, reflected wave, Mars.

I. INTRODUCTION

Although a large amount of observations of the Martian surface in the visible and infra-red domains have been acquired by instruments flown onboard Martian probes or installed onboard the recent NASA rovers, the analyses of returned data have shown that there is a clear need for investigations to better explore and understand the subsurface. Electromagnetic sounding with Ground Penetrating Radars (GPR) appears to be an appropriate method to investigate the geological structures of the Martian subsurface. The MARSIS and SHARAD Radars in orbit around Mars have revealed some impressive structures inside the polar caps but, outside these specific regions, the radar signal seems to undergo such losses that very few echoes coming from the subsurface have been detected.

In the frame of the ESA's ExoMars mission, the Laboratoire Atmosphère, Milieux, Observations Spatiales (LATMOS) - ex Centre d'études des Environnements Terrestres et Planétaires (CETP) has designed and developed a GPR called EISS (Electromagnetic Investigation of the Sub Surface), to sound the deep subsurface of Mars from the surface.

The ExoMars 2013 mission was initially planned with one fixed station and a rover and EISS is designed to take

advantage of the potential for bistatic radar investigations of the planetary subsurface between both stations.

Nevertheless EISS can take advantage of the existence of a single fixed platform to perform monostatic soundings of the subsurface. The ESA Entry, Descent and Landing (EDL) demonstrator may provide in 2016 the next future opportunity for EISS to fly to Mars.

This paper describes the principle of the EISS GPR mainly focusing on its bistatic operating mode. The status of the instrument as well as its end-to-end expected performances is described. Some preliminary validation results are presented about the electrical antenna impedance and about the signal to noise ratio improvement.

II. PRINCIPLE OF THE EISS INSTRUMENT

EISS is a high Frequency (HF) impulse GPR that operates from the surface. The long electrical antenna used to transmit the pulses needs to be deployed on the surface from a fixed platform while the receiver can be either connected to these electrical antennas (for monostatic operations [1],[2],[6]) or to a small magnetic sensor (for bistatic operations) that can be accommodated on a mobile platform like a rover.

In both configurations, the HF frequencies (2MHz or 4MHz) used should allow EISS to perform soundings to kilometric depths. The first level of data processing provides the amplitude and propagation delay associated with the various detected reflectors and interfaces.

While the monostatic mode will give information about the subsurface's structure beneath the Lander, the bistatic mode will give information about the subsurface's structure along the path between the transmitter and the receiver. In bistatic mode, the two signals that travel directly from the transmitter to the receiver above and just beneath the surface are used to estimate the velocity of the wave traveling in the upper layer of the subsurface and to eventually convert the measured delays in distances. This allows one to retrieve the true distance of the reflectors. When soundings are done for different locations of

the receiver, one can build a 2D profile of the subsurface geological structure.

In addition to these radar modes dedicated to the sounding of the subsurface, EISS is also able to give an estimate of the top layer permittivity and conductivity via the HF electrical antenna measured impedance. In passive mode the HF electrical background monitoring also gives information about the electrical activity in the atmosphere and the HF absorption in the ionosphere.

III. INSTRUMENT DESIGN

The following description is similar to the one that was recommended after the first Payload Confirmation Review (PCR) for the ExoMars 2013 mission [5], but several configurations are possible to take advantage of the platforms available for the instrument's units accommodation.

Basically, the EISS instrument is made of two separate units : EISS-GPR1 (both Transmitter and Receiver) which can on its own perform monostatic measurements from the stationary Lander, and EISS-GPR2 (Receiver only) mounted on the Rover that can receive and record the signals reflected by buried structures illuminated by the signal transmitted by EISS-GPR1 (see Figure 1).

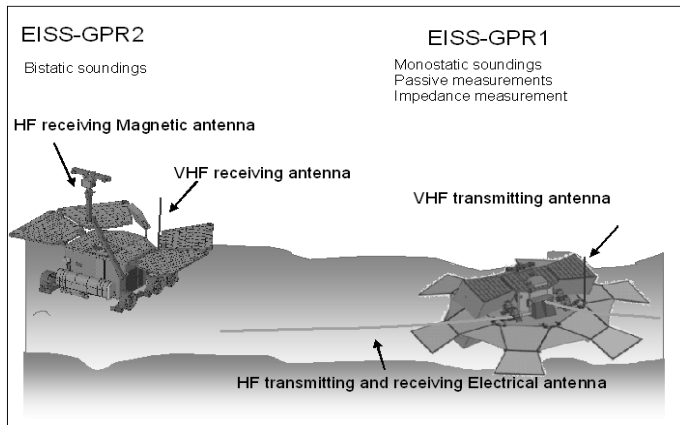


Figure 1. Principle of the EISS instrument on the former ExoMars 2013 mission

EISS-GPR1 uses two 35 meters long electrical loaded monopoles to transmit 10 Watts peak power pulses (5 Watts peak power on each monopole). For soundings down to kilometric depths, the GPR operates with $10\mu\text{s}$ width coded (Binary Phase Shift Keying) pulses with a $80\mu\text{s}$ interpulse period.

The pulse width can be shortened to $1\mu\text{s}$ and even 250ns, allowing shallower soundings, essentially suitable for earthly environment and instrument validation.

EISS-GPR2 magnetic receiver is mounted on the rover possibly on a mast in order to limit the impact of the platform structure on the HF magnetic field and also to rotate the magnetic sensor in order to have access to the three orthogonal components of the magnetic field.

The displacement of the rover over distances of ~ 1 kilometer will allow one to perform successive soundings that will be subsequently analyzed to get a 2D or 3D description of the subsurface structure along the path of the rover. The synchronization between EISS-GPR1 and EISS-GPR2 is ensured by a VHF link operating at 160MHz.

A. Electronic Conception

1) GPR1:

EISS-GPR1 block diagram is shown in Figure 2. There are four main subsystems: HF waveform generation and amplification, HF receiver, VHF transmitter, radar controller and digital unit.

The radar pulses are generated using the direct digital synthesis (DDS) technique. The signal is filtered and amplified up to 10W peak and finally divided between the two differential amplifier outputs. The double pole, double throw (DPDT) switches allow to select one of the two different impedance matching networks for the electrical antenna. The one, dedicated to deep sounding, uses transformers that optimize the transmitted power, but cause distortion of the signal. The other one, purely resistive, is dedicated to shallow soundings and optimizes the impedance matching over the whole bandwidth, but reduces the power transmitted to the antennas. The T/R switches, in off position, protect the HF receiver input during the transmission phase.

After transmission of the signal, the GPR is set to the reception mode (for monostatic measurements), the T/R switches at the input of the HF receiver will select successively each of the two electrical monopoles of the antenna to receive the signal, whereas the 10W amplifier outputs commute on a high impedance load. The HF receiver is constituted of three amplifiers, a band-pass filter and a digital attenuator (4dB steps to 60dB). The amplifiers are used to match the amplitude of the received signal to the ADC scale. If needed, the attenuator reduces the gain of the reception chain to avoid saturation. This together with the fact that coherent additions dramatically improve the signal to noise ratio, allow using the full 12 bits ADC scale (i.e. 72 dB of dynamics) whatever the amplitudes of the received signals are.

The 160MHz oscillator is used as the carrier for the VHF link, and is also used to generate the FPGA clock at 40MHz by means of a divide-by-four prescaler. In bistatic mode, once EISS-GPR2 is synchronized with EISS-GPR1, the command parameters, setting the measurement configuration, are sent before each measurement through the same VHF link using amplitude modulation.

All these functions have been implemented on a single Eurosize card. EISS-GPR1 prototype (form and fit representative of the flight model) also consisted of a second board dedicated to DC/DC conversion to generate all voltages required by EISS-GPR1 electronics from +28V power supply delivered by the platform, which design, development and tests have been subcontracted to Steel Electronics Company.

2) GPR2:

The EISS-GPR2 block diagram is shown in Figure 3. There are three main subsystems: the HF receiver, the VHF receiver, the radar controller and the digital unit. The HF receivers of EISS-GPR1 and EISS-GPR2 are identical. The magnetic sensor provides to the EISS-GPR2 HF receiver's input the HF received signals (the direct ones and the ones reflected by the sub-surface).

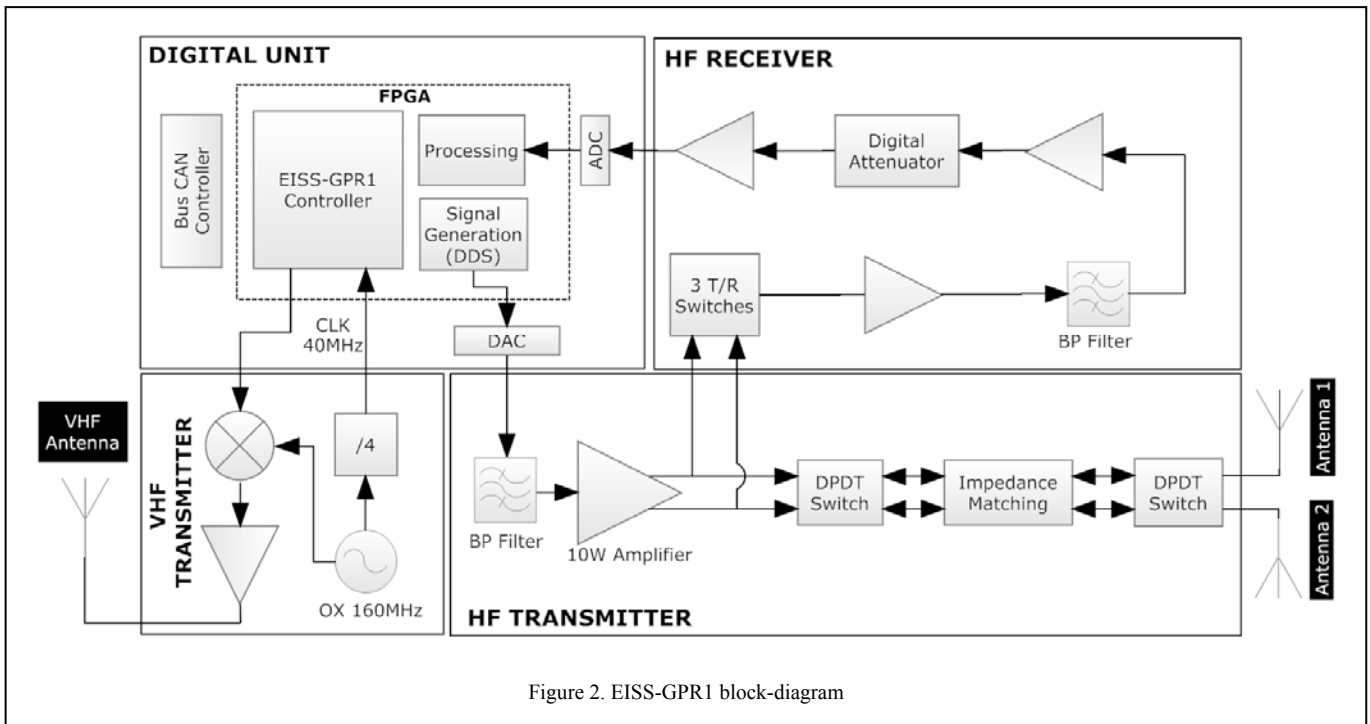


Figure 2. EISS-GPR1 block-diagram

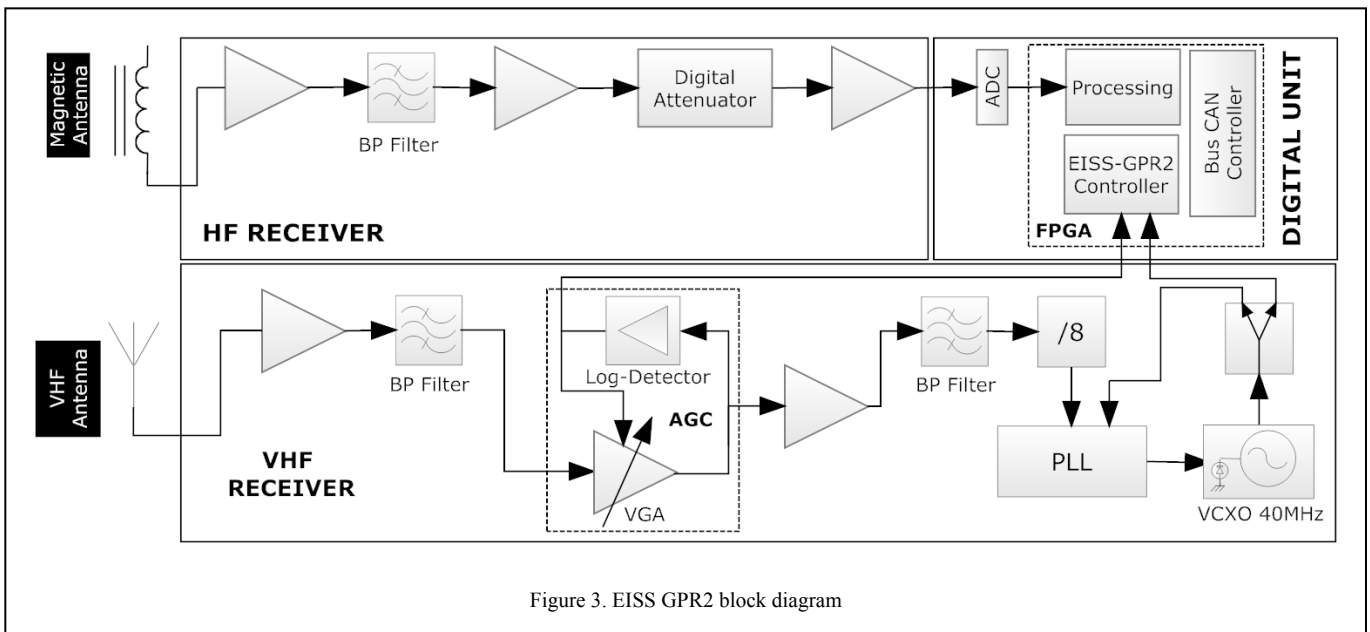


Figure 3. EISS GPR2 block diagram

The VHF receiver is made of two channels. The first one is used for the local oscillator synchronization and the second one is used to set the radar parameters and to trigger the measurement. In order to synchronize the two oscillators, a phase-locked loop (PLL) is used to phase lock the EISS-GPR2 oscillator (40MHz) on the EISS-GPR1 oscillator (160MHz). To ensure a constant level at the input of the PLL, a voltage gain amplifier (VGA) controlled by a logarithmic detector, is used to make an automatic gain control (AGC).

Accurate synchronization of EISS-GPR1 and EISS-GPR2 clocks ($\sim 0.1\text{Hz}$) is crucial to perform bistatic soundings: any larger frequency shift would jeopardize the coherent additions processing which makes it possible to detect weak echoes and get a kilometric penetrating depth.

To set the configuration parameters values in the EISS-GPR2 for each measurement and to start a measurement, the AGC needs to demodulate the signal coming from EISS-GPR1's VHF transmitter. The demodulated signal is obtained from the logarithmic detector's output and is then rescaled to match the inputs level voltage requirement of EISS-GPR2's FPGA. The main characteristics of the instrument are summarized in the following table:

TABLE OF MAIN CHARACTERISTICS OF THE INSTRUMENT

Parameters	GPR1	GPR2	Unit
POWER CHARACTERISTICS			
Voltage Supply	28	28	V
Power Consumption (active modes)	4	4	W
	(1 μ s)	7	W
	(10 μ s)	4	W
Passive mode	3.8		W
TRANSMISSION CHARACTERISTICS			
RF Output (Peak Power)	10		W
Center Frequency	2 / 4		MHz
Pulse Width	0.25/0.5/1/10		μ s
Inter Pulse Period	80		μ s
RECEPTION CHARACTERISTICS			
Frequency Bandwidth	1 - 10		MHz
Maximum Gain	>50		dB
Power Output @ 1dB comp.	14.5		dBm
Number of ADC bits	12		
Sampling Frequency	20		MHz
Attenuator (maximum value)	60		dB
Maximum theoretical dynamic range	132		dB
MECHANICAL CHARACTERISTICS (ANTENNAS EXCLUDED)			
Mass Size	1000	350	g
Length	165	165	mm
Width	105	105	mm
Height	50	45	Mm

B. Descriptions and Characteristics of the antennas

1) Electrical antennas:

EISS needs an HF electrical antenna to transmit the radar signal for both monostatic and bistatic soundings of the subsurface. This antenna will be also used to receive signals in the monostatic and passive operating modes. The electrical antenna size must be commensurate with the wavelength of the radar. At 3 MHz, the wavelength in the vacuum is 100m. Given the constraints of mass and volume of any space mission, the only option for the HF antenna is to use a dipole made of two identical conductive ribbon monopoles that will be coiled during the cruise. This dipole antenna must transmit and receive broadband signals without distortion. To obtain a proper frequency response, the resistivity of each monopole must follow a specific profile along its length. This profile is computed in order to maximize the efficiency of the antenna, to get a suitable impedance value and to avoid distortion of the transmitted pulse [10], [11], [12], [13].

Experimental measurements made on different soils as well as accurate electromagnetic modelling performed with Finite Difference in Time Domain (FDTD) method show that the optimum resistive profile depends on the permittivity of the subsurface upper layer [7], [3]. Since the permittivity of this top layer is not known in advance, the antenna resistive profile needs to be optimised for an *a priori* estimated value ϵ_{r-opt} of the permittivity. However, once on Mars, the antennas will be deployed on a surface having a permittivity value ϵ_{r-soil} that is likely to be different from ϵ_{r-opt} . Simulations have been run to make sure that the chosen resistive profile will ensure for any realistic ϵ_{r-soil} value a reasonable behavior of the antenna. On the other hand, we will show in section IV that this coupling between the electrical antenna and the surface offers an interesting possibility to estimate the permittivity value of the upper subsurface layer.

Each EISS-GPR1 HF electrical monopole antenna is made of Kapton ribbon 24.5 μ m thick, 10mm wide, 34m long. Aluminium metallization on both sides will be made to reach the needed resistive profile. A dielectric layer on each side (~1-3 μ m) will insulate the antenna and provide mechanical protection of the metallic film. To date, use of parylene

coating is being validated by tests. Figure 4 shows a side view of the ribbon layered structure.

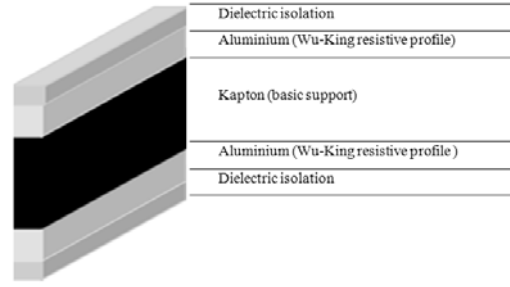


Figure 4. Side view of the ribbon antenna design (vertical exaggeration).

The metallization is sub-contracted to HEF Company. The metallization of the ribbon is obtained by PECVD (Plasma Enhanced Chemical Vapour Deposition) of Aluminium. A software is used to adjust both the scrolling speed of the ribbon facing the Aluminium deposit source and the power applied to the source cathode that controls the Aluminium deposit thickness. The resulting ohmic resistance only depends on this thickness deposit on each section of the ribbon. The parylene insulation process has been worked out and performed by COMELEC Company.

To operate properly the radar, each of the two long HF ribbons monopoles must be deployed on the surface by a dedicated deployment device (see Figure 5). The deployment device has a dual function: the antenna storage and the deployment of the antenna. The mass of the current prototype is less than 90g (antenna mass included), it has been designed, developed and tested by AER Company. The two monopoles are deployed on the surface in nearly opposite directions, at an angle which, when EISS is used in bistatic mode, ensures good volume coverage around the transmitter.

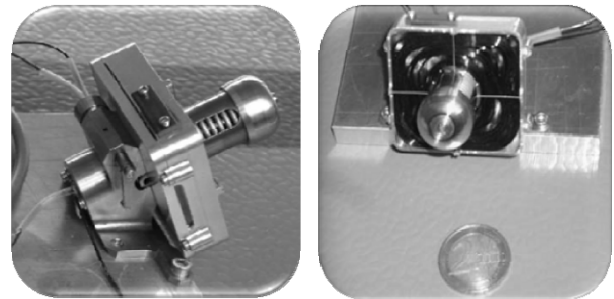


Figure 5. Deployment device of HF ribbons antennas.

2) Magnetic antenna:

EISS's most innovative capability is its potential for bistatic operation, made possible by the use of a small magnetic sensor on the receiver which can measure the magnetic field (all 3 components) of each received HF wave, whatever the direction and orientation of the mobile station.

The magnetic antenna operates at a center frequency F_0 of 3MHz over a 1-6MHz bandwidth, with a sensitivity at $F_0 \pm 0.4$ MHz equal to $2fT/\sqrt{Hz}$ and a gain equals to 40dB.

The antenna is made of four units: the ferrite core (Nickel Zinc), the primary and secondary windings, the pre amplifier and the calibration network. The antenna weights 80g and the dimensions of the mechanical housing are 110x22x35mm. Figure 6 shows a magnetic antenna's picture.

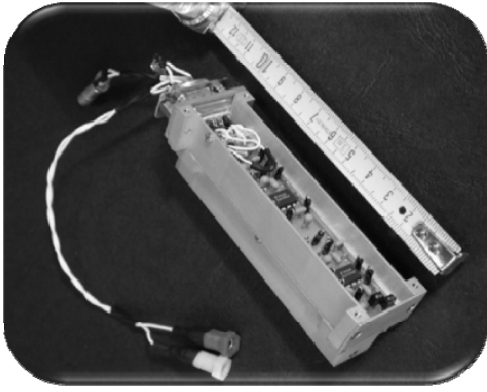


Figure 6. Picture of the magnetic antenna.

The primary winding generates an induced voltage proportional to the magnetic field to be measured. The secondary winding is a flux feedback network. It is used to improve the antenna bandwidth and to reach a satisfying tradeoff between the gain and the bandwidth (see Figure 7). The calibration network is used to check that the antenna is operating with its nominal performances.

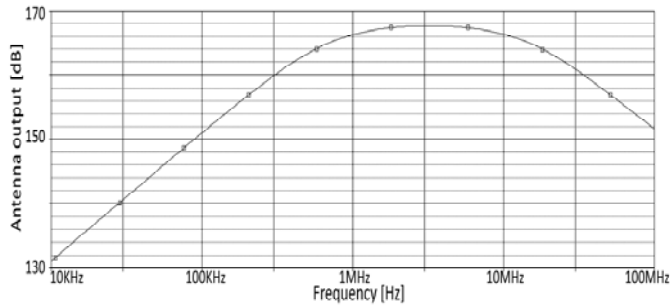


Figure 7. Antenna output with flux feedback as a function of frequency

The ferrite core's shape has been optimized to maximize the magnetic induction inside the core [9]. Several numerical simulations with the Flux 2D software have been performed to study the impact of this shape. Figure 8 shows the magnetic induction inside the core as a function of the core length for two shapes cases : shape 1 is a perfect cylinder while shape 2 is optimized by thinning down its central part. Shape 2, used for the design of EISS magnetic antenna, provides a magnetic amplification three times higher than Shape 1. This result clearly shows the impact of the core shape and the need to optimize it.

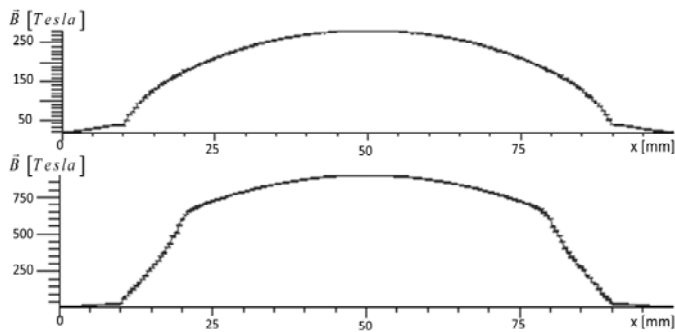


Figure 8. Magnetic induction inside the ferrite core for two different ferrite shapes as a function of the core length. The results have been obtained through accurate electromagnetic simulations with the finite element software Flux 2D.

3) VHF antenna:

Operation of the bistatic mode requires that the 2 modules GPR1 and GPR2 are synchronized. This synchronization is achieved with the VHF link between both platforms. A VHF subsystem is accommodated on each module: Transmitter on GPR1, Receiver on GPR2 with a VHF antenna on both sides.

The frequency value has been chosen according to the mission constraints: the minimization of the instrument size and mass, the frequencies already used on the platforms, the accommodation of the VHF antennas as high as possible on both platforms and especially a link range of at least 1km. At the moment, to meet all these requirements, we chose to operate at 160MHz with a $\lambda/4$ monopole made of a thin and very elastic metallized carbon fiber rod (46cm length, 0.5mm diameter, 2g for monopole only, 30g with connectors and mounting hardware). The obtained 3D antenna pattern is relatively omnidirectional even in the presence of the platforms with a maximum gain of 2dB.

The main part of the VHF link antenna, the carbon rod, will be provided by the subcontractor INVENT GmbH in Braunschweig / Germany.

IV. EXPERIMENTAL VALIDATION OF THE INSTRUMENT

The assessment of the EISS performances is ongoing using numerical FDTD simulations together with data processing algorithms. Laboratory and field tests have also been initiated to determine the performances of each operating mode and to prepare data interpretation.

1) Impedance measurement:

The subsurface survey requires knowledge of the permittivity of the studied sub-surface layers to accurately convert the measured propagation delays into distances. Access to electrical characteristics of ground that EISS is able to provide without return samples or *in situ* analysis, is unusual in space missions and aroused great interest.

As already mentioned, when the EISS electrical antenna is deployed on the surface, a significant electromagnetic coupling with the subsurface top layer occurs. As a result, the antenna impedance seen by the radar depends on the subsurface upper layer permittivity and conductivity and can be used to retrieve these characteristics.

Simulations have been run for the antenna optimized for a ϵ_{r-opt} value of 4 to quantify the effect of the permittivity value ϵ_{r-soil} and the conductivity value σ of the subsurface. They show (see Figure 9) that the conductivity value σ has an impact only at frequencies below 1.5MHz and that, as a consequence, the higher frequencies of the bandwidth (>3MHz) can be used to estimate the permittivity value ϵ_{r-soil} .

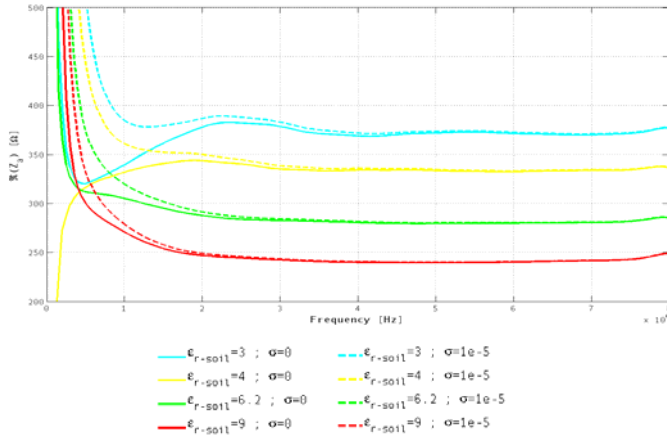


Figure 9. Variation of the real part of the electrical antenna impedance as a function of the frequency for different values of the subsurface permittivity. The variation of conductivity has a noticeable effect only below 1.5 MHz.

Measurements performed on dry sand in the forest of Fontainebleau (see Figure 10) validated this principle of data inversion. From the impedance measurements, the electrical properties of the sand have been estimated to be $\epsilon_{r\text{-soil}}=4$ and $\sigma=5.10^{-5} \text{ S.m}^{-1}$ which are in reasonable agreement with results found in the literature.

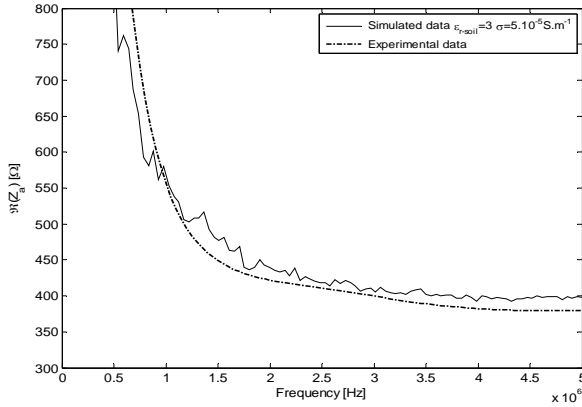


Figure 9. Comparison between simulated and measured antenna impedance.

2) Subsurface sounding mode

At reception, the recorded echoes are masked by the noise. To improve the detection of echoes corresponding to direct or reflected waves, coherent summations have been implemented. The probed subsurface and the characteristics of the transmitted signal being invariant during the measurement time, the echoes received are coherent, unlike the noise which is random, uncorrelated and independent of data. N coherent additions theoretically induce a multiplication of the useful signal by N and of the uncorrelated noise by \sqrt{N} and thus a significant improvement of the signal to noise ratio (SNR). The current prototype of the radar is able to carry up to 2^{31} coherent additions that would improve in the best case the SNR by 93 dB. On the other side, the power consumption of the instrument and the acquisition time of measurement are increased, for example 2^{26} additions require 10 minutes. Figure 10 shows the significant improvement of signal to noise ratio provided by the coherent additions.

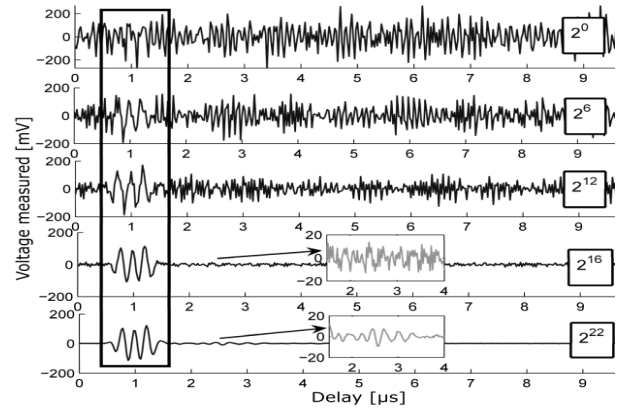


Figure 10. Effect of coherent additions on the signal to noise ratio. These measurements were made on the Dune du Pyla in bistatic mode. The transmitter and receiver were separated by 130m. [8].

Experimental validation of the instrument bistatic principle has been performed in the Egyptian desert with a previous version of the instrument [4] that used GPS signal for the synchronization of both oscillators instead of the VHF link. The preliminary results obtained show that reflecting structures located at an approximate depth of 150 and 200 meters were detected. (Figure 11)

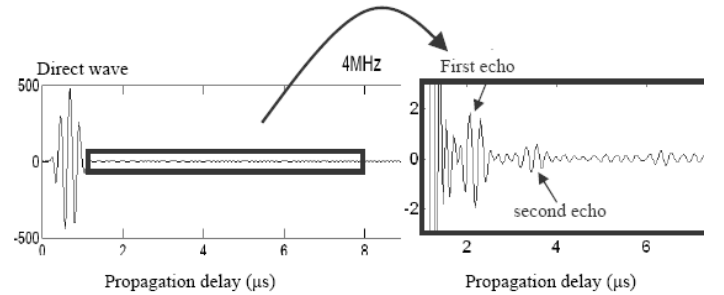


Figure 11. Example of received echoes detected by a prototype of the EISS magnetic antenna in bistatic configuration.

V. CONCLUSION

All EISS's subsystems described in this paper: EISS-GPR1 electronics, electrical ribbon antennas and associated deployment system, VHF antennas, EISS-GPR2 electronics and magnetic antenna have been designed, manufactured and tested in their "flight representative" form in accordance with the stringent constraints of a space mission in terms of mass (1.1kg for EISS-GPR1 and 330g for EISS-GPR2 in ExoMars 2013 configuration), size and power consumption. Components quality, mechanical, thermal and radiation environments, cleanliness and planetary protection requirements have also been taken into account early in the design so that a clear path has been defined to go from the form and fit representative prototype to the qualification and flight models of the instrument.

VI. FUTURE PLANS

The performances of the VHF link designed for EISS which is used to remotely synchronize the local oscillators on both units of the instrument, set the parameters values for each sounding and trigger the measurement will be soon experimentally assessed. Particular attention will be paid to the

maximum distance that can be achieved between the transmitter and the receiver.

Once the VHF link performances are nominal, the experimental validation of the whole EISS instrument will have to be done. Well documented sites showing identified buried structures with reasonable conductivity in order to get good penetration need to be selected in both arid and cold environments.

The ExoMars mission has recently undergone a complete redesign and the stationary platform and its whole payload has been removed from the new 2018 mission. Nevertheless opportunities to use the EISS GPR on Earth (to search for deep liquid water reservoirs in arid environments for example or to map the bed-rock buried under thick layers of ice...) or on future planetary missions will not be missed

ACKNOWLEDGMENT

The development and validation of the instrument is funded by CNES

REFERENCES

- [1] Berthelier J. J., Ney R., Ciarletti V., Martinat B., Hamelin M., Costard F., Paillou P., Nevejans C., Kofman W., Trotignon J. G., Grandjean G., Zamora M., and Nagy A. (2003). GPR, a ground-penetrating radar for the NetLander mission. *Journal of Geophysical Research*, 108(E4) :8027, doi :10.1029/2002JE001866.
- [2] Berthelier J. J., Ney R., Costard F., Meyer A., Martinat B., Reineix A., Hansen T., Bano M., Kofman W., Lefeuvre F., and Paillou P. (2000b). The GPR experiment on NetLander. *Planetary and Space Science*, 48 :1161–1180.
- [3] Biancheri-Astier M., Ciarletti V., Reineix A., Corbel C. (2010). Optimization of resistive profile for loaded electrical monopole dedicated to deep Martian subsurface sounding. (submitted to *Journal of Geophysical Research*)
- [4] Ciarletti V., Le Gall A., Berthelier J. J., Corbel C., Dolon F., Ney R., Reineix A., Guiffaut C., Clifford S., Heggy E., (2007). Bi-static deep electromagnetic soundings for martian subsurface characterization: Experimental validation in the Egyptian Western desert. *Lunar and Planetary Science XXXVIII*
- [5] Grassl et al, Payload Confirmation Review (PCR) Board Report, EXM-MS-RP-ESA-00005, Issue: 1, 28 March 2007
- [6] Le Gall A., Ciarletti V., Berthelier J. J., Reineix A., Guiffaut C., Ney R., Dolon F., and Bonaimé S. (2008). An imaging HF GPR using Stationary Antennas: Experimental Validation over the Antarctic Ice Sheet. *IEEE Trans Geoscience and Remote Sensing*. *IEEE Transactions on Geoscience and Remote Sensing*, vol. 46, issue 12, pp. 3975-3986 doi: 10.1109/TGRS.2008.2000718
- [7] Le Gall A., Reineix A., Ciarletti V., Berthelier J. J., Ney R., Dolon F., and Corbel C. (2006). An estimation of the electrical characteristics of planetary shallow subsurfaces with TAPIR antennas. *Journal of Geophysical Research*, 111(E06S06), doi :10.1029/2005JE002595.
- [8] Le Gall A. (2007). Sondage des sous-sols planétaires par radar à pénétration de sol : Etude et modélisation des performances de l'instrument TAPIR. PhD thesis, CETP Centre d'études des Environnement terrestre et planétaires.
- [9] Leroy P., Coillot C., Roux A., Chanteur G (2006). Optimization of the Shape of Magnetic Field Concentrators to Improve the Sensitivity of Hall Sensors. *Techniques de l'Ingénieur*, Volume73, Issue6 : 339-349.
- [10] Wait J. R. (1972). Theory of wave propagation along a thin wire parallel to an interface. *Radio Science*, 7(6) :675–679.
- [11] Wright D. L. and Prewitt J. F. (1975). A radiating dipole antenna with tapered impedance loading. *IEEE Trans. Antennas Propag.*, 23(11) :811–814.
- [12] Wu T. T. and King R.W. P. (1965). The cylindrical antenna with nonreflecting resistive loading. *IEEE Trans. on Antenna Propagation*, 13 :369–373.
- [13] Wu T. T. and Shen L. S. (1967). Cylindrical antenna with tapered resistive loading. *Radio Science*, 2(2) :191–201.